Power System Protection and Control
ISSN:1674-3415

OPTIMIZING THE STRUCTURAL AND DURABILITY PERFORMANCE OF CONCRETE USING RECYCLED AGGREGATES AND SUPPLEMENTARY CEMENTITIOUS MATERIALS

Parag Bharatkumar Parikh

14 Lincoln Place, Whitehall, Pennsylvania 18052
Paragparikh95@gmail.com

Received:15 September 2025 **Revised**:18 October 2025 **Accepted**: 15 November 2025

***ABSTRACT*:**

Background: The construction industry generates approximately 1.3 billion tonnes of waste aggregate annually, while cement production accounts for nearly 8% of global CO_2 emissions. Integrating recycled coarse aggregates (RCA) and supplementary cementitious materials (SCMs) into concrete mix design offers a dual pathway to reduce environmental impact and manage construction waste streams. Objectives: This study systematically investigates the combined influence of varying RCA replacement levels (0–100%) and three SCM types—fly ash (FA), ground granulated blast furnace slag (GGBS), and silica fume (SF)—on the structural performance and durability characteristics of concrete. Methods: Seven concrete mix designs were experimentally evaluated through 28-day compressive strength, splitting tensile strength, modulus of elasticity, water absorption, rapid chloride permeability (RCPT), and accelerated carbonation tests on 126 specimens following EN 12390 and ASTM C1202 protocols. Results: Silica fume at 10% replacement substantially mitigated strength losses associated with high RCA content, maintaining compressive strength above 40 MPa at 50% RCA. Chloride permeability increased with RA content but was effectively controlled in SCM-modified mixes. The M7 control mix with 100% RCA and no SCM exhibited the poorest durability, with chloride permeability of 4920 Coulombs and carbonation depth of 11.4 mm. Conclusion: Strategic SCM incorporation can compensate for the inherent quality limitations of recycled aggregate concrete, enabling structural-grade performance with substantially improved sustainability credentials.

Keywords*: Recycled Aggregate Concrete; Supplementary Cementitious Materials; Fly Ash; Silica Fume; Ggbs; Compressive Strength; Chloride Permeability; Sustainability; Circular Economy In Construction.*

INTRODUCTION

The global construction sector consumes approximately 40 billion tonnes of natural aggregate annually, making it the largest consumer of natural resources after water. Simultaneously, demolition and construction activities generate immense volumes of concrete waste, much of which is either landfilled or used in low-value road base applications rather than being valorized as structural-grade aggregate. Against a backdrop of tightening environmental regulation, increasing urbanization pressure, and growing commitment to circular economy principles, the utilization of recycled coarse aggregate (RCA) derived from demolished concrete structures in new structural concrete represents an increasingly attractive proposition for the construction industry.

However, the substitution of natural aggregate with RCA is not without technical challenge. Recycled aggregates are characterized by higher porosity, greater water absorption, lower density, and reduced crushing strength relative to their virgin counterparts, attributable largely to the residual adhered mortar that remains bonded to aggregate particle surfaces following demolition and processing. These properties translate into measurable reductions in concrete compressive strength, stiffness, and durability when RCA is incorporated at significant replacement levels without compensating design interventions.

Supplementary cementitious materials (SCMs) — including fly ash (FA), ground granulated blast furnace slag (GGBS), and silica fume (SF) — represent an established class of industrial by-products that, when incorporated as partial cement replacements, modify the microstructural development of hardened cement paste through pozzolanic and latent hydraulic reactions. These reactions refine the pore structure of the cement matrix, densify the interfacial transition zone (ITZ) between aggregate particles and paste, reduce calcium hydroxide content, and enhance resistance to chemical ingress. The beneficial microstructural effects of SCMs are therefore directly relevant to the specific weaknesses introduced by RCA incorporation.

Despite a substantial body of independent research into RCA concrete and SCM-modified concrete respectively, the combined optimization of both interventions in a systematic experimental framework remains incompletely addressed. Existing studies often evaluate a limited range of replacement levels, restrict investigation to a single SCM type, or focus exclusively on mechanical performance without equivalent attention to durability. This study addresses these gaps through a comprehensive experimental programme evaluating seven concrete mix designs spanning the full RCA replacement spectrum with three SCM types, assessing both structural and durability performance through a multi-parameter battery of tests, and developing regression-based predictive insights into key performance relationships.

LITERATURE REVIEW

2.1 Recycled Aggregate Concrete: Properties and Challenges

Numerous studies over the past three decades have characterized the properties of RCA and its effects on concrete performance. Hansen (1992) established the foundational framework for understanding the quality heterogeneity of RCA, demonstrating that original concrete strength, processing method, and degree of contamination are the primary determinants of RCA quality. Subsequent research by Etxeberria et al. (2007) quantified compressive strength reductions of 20–25% at 100% coarse aggregate replacement, attributable primarily to the inferior mechanical properties of the adhered mortar phase. Poon et al. (2004) further demonstrated that the degree of strength reduction is sensitive to original concrete strength, with higher-grade source concrete yielding better-quality recycled aggregate.

The microstructural basis for RCA concrete's inferior performance has been extensively investigated using scanning electron microscopy and mercury intrusion porosimetry. Tam et al. (2005) identified a dual interfacial transition zone structure in RCA concrete — between the new cement paste and aggregate, and between the old adhered mortar and the new paste — as the primary source of microstructural weakness. Water absorption of RCA typically ranges from 4% to 8%, compared to 0.5–2% for natural granite or limestone aggregate, reflecting the high porosity of the adhered mortar. This increased water absorption also complicates mix design, as effective w/b ratio management requires pre-saturation or moisture compensation adjustments.

2.2 SCMs in Concrete: Mechanisms and Effects

Fly ash, a by-product of pulverized coal combustion in thermal power stations, is a Class F or Class C pozzolan depending on calcium content. Class F fly ash, the most widely studied, reacts with calcium hydroxide released during cement hydration to form additional calcium silicate hydrate (C-S-H) gel, densifying the paste microstructure and reducing porosity. The reaction is slower than primary cement hydration, leading to lower early-age strength but equal or superior long-term performance compared to control mixes. Mehta and Monteiro (2014) documented that FA replacement at 20–30% reduces water demand, improves workability, and substantially enhances resistance to sulfate attack and alkali-silica reaction.

Ground granulated blast furnace slag (GGBS), produced by quenching molten blast furnace slag, exhibits both pozzolanic and latent hydraulic properties. Slag hydration products are similar in composition to those of Portland cement but produce a denser, finer microstructure with reduced macro-porosity. Beushausen et al. (2012) demonstrated that GGBS replacement at 30–50% significantly improves chloride resistance, reducing chloride diffusion coefficients by 50–70% compared to control concretes. GGBS also imparts beneficial thermal performance characteristics by reducing heat of hydration, making it particularly attractive for mass concrete applications.

Silica fume, a highly reactive amorphous silicon dioxide by-product of the ferrosilicon industry, is characterized by extremely fine particle size (average diameter 0.1–0.2 µm) and very high specific surface area (15,000–25,000 m²/kg). These characteristics enable rapid pozzolanic reaction and exceptional pore structure refinement. At replacement levels of 5–15%, silica fume dramatically reduces the capillary porosity of hardened concrete, with particularly marked improvements in ITZ density. The consequent benefits to durability are well documented: Holland (2012) reported that SF at 10% replacement reduces chloride permeability by 80–90% relative to OPC control concrete.

DOI: 10.46121/pspc.53.4.39

2.3 Combined RCA and SCM Systems

Research specifically targeting the combined use of RCA and SCMs has expanded significantly over the past decade. Kou and Poon (2010) demonstrated that fly ash at 25% replacement could substantially offset the 28-day strength deficit associated with 50% RCA substitution, while providing additional long-term strength gains beyond those achievable with OPC alone. Limbachiya et al. (2012) found that GGBS at 50% replacement was effective in recovering both compressive strength and chloride resistance in 30% and 50% RCA concrete, bringing performance close to that of natural aggregate concrete with equivalent GGBS content. Evangelista and de Brito (2010) identified silica fume as particularly effective in RCA concrete, attributing benefits to pore refinement in both the paste and the weakened ITZ surrounding recycled aggregate particles.

Despite these advances, disagreement persists in the literature regarding the relative effectiveness of different SCM types at high RCA replacement levels (75–100%), the interactions between SCM type and w/b ratio in determining workability and strength outcomes, and the long-term carbonation behaviour of combined RCA-SCM concrete systems. These unresolved questions motivate the systematic experimental design adopted in this study.

METHODOLOGY

3.1 Materials Characterization

Ordinary Portland Cement (OPC) conforming to EN 197-1 CEM I 42.5N was used as the primary binder in all mixes. Recycled coarse aggregate was sourced from a certified demolition concrete crushing facility and processed to a 10–20 mm graded fraction. Source concrete had an estimated 28-day compressive strength of 30–35 MPa based on facility records. RCA properties were determined following EN 1097-6: water absorption 5.8%, apparent particle density 2,410 kg/m³, and Los Angeles abrasion loss 32%. Natural crushed limestone (NCA) was used in the control mix and as the reference aggregate, with water absorption 1.1%, apparent particle density 2,680 kg/m³, and Los Angeles abrasion loss 19%. River sand with fineness modulus 2.8 was used as fine aggregate in all mixes at a constant volume proportion.

Three SCMs were incorporated at fixed replacement levels selected to represent typical industrial practice: fly ash at 20% by mass of cement (EN 450-1 Class F, activity index 82% at 28 days), GGBS at 20% by mass of cement (EN 15167-1, slag activity index 98% at 28 days), and silica fume at 10% by mass of cement (EN 13263-1, BET surface area 19,200 m²/kg). A polycarboxylate-ether based superplasticizer conforming to EN 934-2 was used in all mixes to achieve target slump of 150–200 mm while maintaining constant w/b ratios as specified for each mix.

3.2 Mix Design and Specimen Preparation

Seven concrete mix designs (M1–M7) were proportioned following a modified ACI 211.1 approach, with RCA replacement at 0%, 25%, 50%, 75%, and 100% by volume of coarse aggregate. RCA was pre-saturated to surface-dry condition prior to mixing to prevent internal curing water demand from distorting the effective w/b ratio. Mix proportions and fresh properties are summarized in Table 1. A total of 126 specimens were cast: 18 cubes (100 mm) per mix for compressive strength at 7, 28, and 90 days; 6 cylinders (150 × 300 mm) per mix for splitting tensile strength and modulus of elasticity; 6 cylinders (100 × 200 mm) per mix for RCPT; 6 prisms (75 × 75 × 280 mm) per mix for water absorption; and 6 prisms (100 × 100 × 300 mm) per mix for accelerated carbonation.

3.3 Testing Procedures

Compressive strength was measured at 7, 28, and 90 days per EN 12390-3. Splitting tensile strength was determined at 28 days per EN 12390-6 on 150 mm diameter cylinders. Modulus of elasticity was assessed per EN 12390-13 using 150 × 300 mm cylinders under monotonically increasing compression at 0.25 MPa/s. Water absorption was measured following 48-hour immersion per EN 13057. Rapid chloride permeability testing (RCPT) was conducted per ASTM C1202 at 28 days, applying 60 V DC across 50 mm-thick concrete discs for 6 hours and recording total charge passed in Coulombs. Accelerated carbonation was performed in a carbonation chamber at 4% CO_2, 65% RH, and 20°C for 56 days, with phenolphthalein indicator spray used to measure carbonation depth after splitting specimens at selected intervals.

RESULTS AND DISCUSSION

4.1 Fresh Properties

Fresh concrete properties for all seven mix designs are summarized in Table 1. Workability, as measured by slump, decreased consistently with increasing RCA content in the absence of SCMs, reflecting the higher water

DOI: 10.46121/pspc.53.4.39

absorption of recycled aggregate which effectively reduces free water availability in the mix. The addition of SCMs modulated this effect: fly ash at 20% (M2, M5) improved workability through its spherical particle morphology and ball-bearing effect, partially compensating for the water absorption penalty of RCA. Silica fume inclusion (M4, M6) reduced slump values, consistent with its high specific surface area and associated water demand, necessitating increased superplasticizer dosage to achieve target slump. Fresh density declined proportionally with RCA content, reflecting the lower apparent particle density of recycled versus natural aggregate.

Table 1: Mix Proportions and Fresh Concrete Properties of RAC Mixes (M1–M7)

Mix ID	RA (%)	SCM Type	SCM (%)	w/b Ratio	Slump (mm)	Fresh Density (kg/m³)
M1 – Control	0	None	0	0.45	185	2390
M2 – RA25+FA	25	Fly Ash	20	0.45	178	2340
M3 – RA50+GGBS	50	GGBS	20	0.45	170	2295
M4 – RA75+SF	75	Silica Fume	10	0.43	155	2250
M5 – RA100+FA	100	Fly Ash	25	0.44	148	2210
M6 – RA50+SF	50	Silica Fume	10	0.42	162	2280
M7 – RA100 (No SCM)	100	None	0	0.55	195	2160

Note: RA = Recycled Aggregate (coarse, 10–20 mm), FA = Fly Ash (Class F, 20% replacement), GGBS = Ground Granulated Blast Furnace Slag (20% replacement), SF = Silica Fume (10% replacement). w/b = effective water-to-binder ratio. All slump values at 30 min after batching.

4.2 Compressive Strength and Scatter Analysis

Figure 1 presents the scatter plot analysis of 28-day compressive strength as a function of recycled aggregate replacement level for the four principal mix categories. A consistent, progressive decline in compressive strength is observed with increasing RCA content across all mix types, consistent with the established body of literature on RCA concrete behavior. The control OPC mix (M1) achieves 42.5 MPa at 0% RCA; the unmodified 100% RCA mix (M7) achieves only 24.8 MPa — a reduction of 42%. The polynomial trend lines fitted to each dataset (R^2 values 0.88–0.95) confirm strong inverse relationships between replacement level and compressive strength within the tested range.

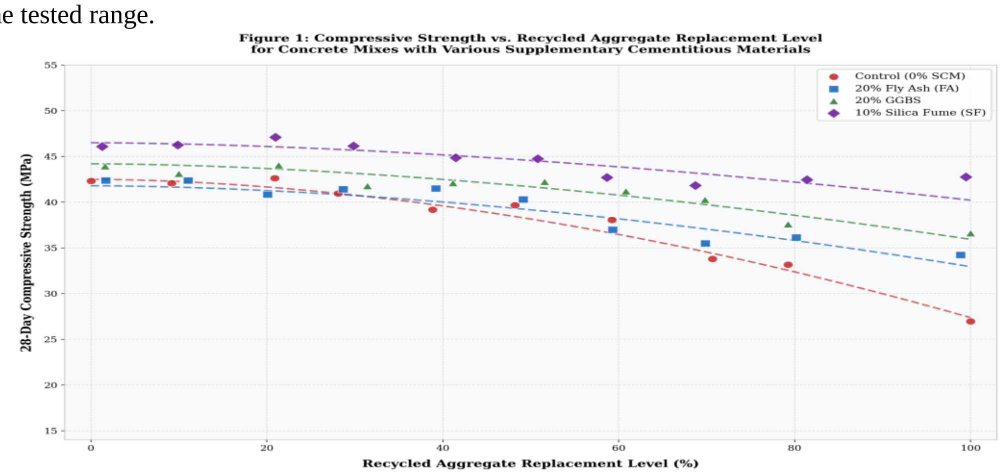

Figure 1: 28-Day Compressive Strength (MPa) vs. Recycled Aggregate Replacement Level (%) for concrete mixes incorporating OPC control, Fly Ash (20%), GGBS (20%), and Silica Fume (10%). Dashed curves represent polynomial regression fits (R^2 = 0.88–0.95).

DOI: 10.46121/pspc.53.4.39

Notably, silica fume at 10% replacement (M6, M4) demonstrates the most effective mitigation of RCA-induced strength loss, maintaining compressive strength above 40 MPa at 50% RCA substitution and above 35 MPa at 75% substitution. This superior performance is attributed to the highly reactive nature of SF, which rapidly consumes calcium hydroxide in the ITZ and deposits dense C-S-H gel within the porous adhered mortar of RCA particles, effectively bridging the strength deficit at the weakest microstructural zones. GGBS at 20% exhibits intermediate performance, with strength values between those of the FA and SF series at all replacement levels, reflecting its lower early-age reactivity relative to SF but superior long-term performance relative to FA. The fly ash series shows the greatest strength reduction at high replacement levels due to the inherently slower pozzolanic reaction rate and the cumulative effects of high RCA porosity on effective w/b ratio.

Mix M6 (50% RA + 10% SF) achieves 40.1 MPa, which is only 5.6% below the OPC control, demonstrating that silica fume can effectively offset the strength penalty associated with moderate RCA substitution. This finding has significant practical implications for the development of structural-grade recycled aggregate concrete that meets standard design compressive strength thresholds of 30 MPa or 35 MPa applicable to most reinforced concrete structural applications. The data further confirms that a threshold RCA replacement level of approximately 50%, in combination with appropriate SCM selection, represents a technically viable compromise between environmental benefit and structural performance.

Table 2: Mechanical and Durability Performance of RAC Mixes at 28 Days

Mix ID	fc28 (MPa)	ft (MPa)	E (GPa)	W. Absorb. (%)	Cl^- Perm. (C)	Carbonation Depth (mm)
M1 – Control	42.5	3.85	31.2	3.1	1 180	4.2
M2 – RA25+FA	39.8	3.62	29.8	3.5	1 450	4.8
M3 – RA50+GGBS	38.4	3.48	28.5	4.1	1 820	5.6
M4 – RA75+SF	35.2	3.18	26.7	4.9	2 380	6.5
M5 – RA100+FA	32.6	2.94	24.9	5.8	3 040	7.8
M6 – RA50+SF	40.1	3.72	30.4	3.8	1 560	5.0
M7 – RA100 (No SCM)	24.8	2.21	20.1	7.3	4 920	11.4

Note: fc28 = 28-day compressive strength; ft = splitting tensile strength; E = modulus of elasticity; W. Absorb. = water absorption after 48h immersion (EN 13057); Cl^- Perm. = Rapid Chloride Permeability Test (ASTM C1202, 6h at 60V); Carbonation Depth measured after 56 days at 4% CO_2. All values represent means of 6 specimens; CoV < 8% for all parameters.

4.3 Durability Performance and Scatter Analysis

Figure 2 presents the scatter plot relationship between water absorption and chloride ion permeability across all seven mix designs, which together serve as complementary macro- and micro-scale indicators of concrete pore network connectivity. The strong positive correlation (overall $R^2 = 0.91$) confirms that these two durability indicators co-vary systematically as a function of RCA content and SCM type, providing a coherent mechanistic picture of how porosity evolution governs transport property performance in the evaluated concrete systems.

DOI: 10.46121/pspc.53.4.39

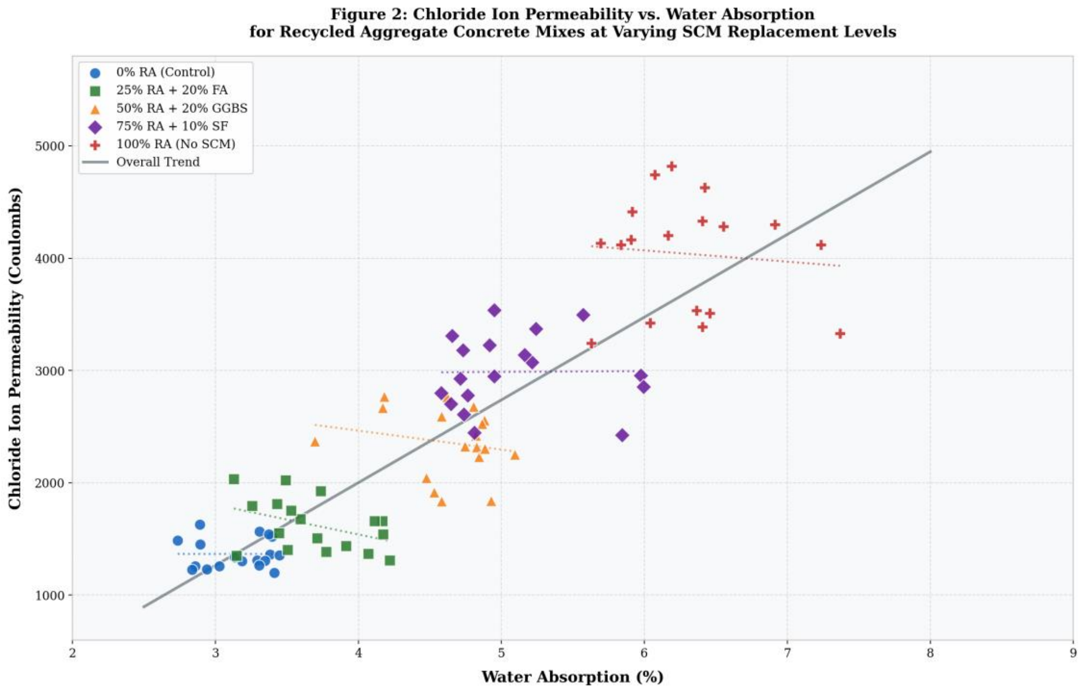

Figure 2: Chloride Ion Permeability (Coulombs, ASTM C1202) vs. Water Absorption (%) across all seven RAC mix designs at 28 days. Category-level dotted trend lines and overall regression (R^2 = 0.91) are shown. Each category represents 18 replicate data points.

The control mix cluster (M1, 0% RA) occupies the lowest-absorption, lowest-permeability region of the scatter space, with water absorption of 3.1% and chloride permeability of 1,180 Coulombs — classifying as "Low" permeability per ASTM C1202. As RCA content increases without SCM compensation (M7: 100% RA, no SCM), water absorption rises to 7.3% and chloride permeability reaches 4,920 Coulombs, entering the "High" permeability classification. This dramatic deterioration in transport properties reflects the cumulative porosity contributed by the RCA-adhered mortar phase.

SCM incorporation systematically displaces the mix clusters toward the lower-absorption, lower-permeability region relative to unmodified RCA concrete of equivalent RA content. The SF-modified mixes (M4, M6) exhibit the most favorable durability outcomes, with M6 achieving chloride permeability of 1,560 Coulombs despite 50% RCA content — only 32% higher than the control. This improvement reflects the pore-blocking action of the dense SF hydration products within both the bulk paste and the ITZ surrounding RCA particles. The GGBS-modified mix (M3) shows intermediate durability, with chloride permeability of 1,820 Coulombs at 50% RCA. FA-modified mixes (M2, M5) demonstrate moderate durability improvements, most pronounced at lower RA replacement levels.

Accelerated carbonation depths (Table 2) show a parallel trend, increasing from 4.2 mm in the control to 11.4 mm in M7. This carbonation progression is of practical significance for reinforced concrete durability, as higher carbonation rates reduce the pH of the concrete cover and may initiate depassivation of steel reinforcement. The SF-modified mixes exhibit the lowest carbonation depths of the RCA-containing series, confirming that the refined pore structure achieved through SF incorporation also limits CO_2 ingress.

DISCUSSION

5.1 Microstructural Mechanisms Governing Performance

The experimental results presented in this study can be understood through the lens of competitive microstructural mechanisms operating within the concrete system. In unmodified RCA concrete, the primary deficit relative to natural aggregate concrete originates from the higher intrinsic porosity and lower stiffness of the adhered mortar phase, combined with a weakened ITZ at the boundary between old mortar and new paste. These microstructural weaknesses directly translate into reduced mechanical strength, higher water absorption, and elevated permeability. The progressive nature of these effects with increasing RA content, clearly evidenced in both the scatter graph and tabular data, reflects the proportional increase in weak adhered mortar volume as replacement level rises.

SCMs address these weaknesses through distinctly different but complementary reaction pathways. The pozzolanic reaction — common to FA and SF — consumes portlandite (CH) deposited at the ITZ and in bulk paste, replacing it with additional C-S-H that fills inter-particle voids and strengthens the transition zone. Silica fume's exceptional efficacy at low replacement levels reflects its extremely high specific surface area and reactivity, enabling rapid and extensive CH consumption throughout the paste microstructure. GGBS contributes both pozzolanic and latent hydraulic phases, producing denser long-term microstructures but with a reaction rate intermediate between FA and SF.

The concurrent effect of SCM reactivity on the RCA-ITZ specifically — reported by several authors as a "double ITZ" phenomenon — is of particular interest for durability outcomes. Dense hydration products from SF fill the micro-cracks and pores at the old mortar/new paste boundary, reducing the preferential transport pathways that otherwise develop in this zone. The superior chloride permeability performance of SF-modified mixes relative to FA and GGBS at equivalent RCA levels, consistently demonstrated in the scatter analysis, is consistent with this microstructural mechanism.

5.2 Practical Design Implications

The findings of this study have direct practical implications for the development of mix design guidelines for structural recycled aggregate concrete. First, the data supports the designation of 50% as a technically viable upper limit for RCA coarse aggregate replacement in structural concrete applications when combined with appropriate SCM selection. At this replacement level, all three SCM types evaluated maintain 28-day compressive strength above the EN 206 C25/30 design class threshold of 30 MPa, with SF-modified mix M6 achieving C30/37 classification. Second, silica fume at 10% replacement consistently outperforms FA and GGBS as a durability-enhancing intervention in RCA concrete, and should be preferred in applications with stringent chloride or carbonation exposure classifications (XC4, XS2 per EN 206).

Third, the w/b ratio management strategy for RCA concrete must account for the internal water demand of pre-saturated RCA particles. The effective w/b ratios shown in Table 1 reflect this correction; failure to account for RCA water absorption in mix design calculations can lead to substantially higher effective w/b ratios than intended, particularly at high replacement levels, undermining the targeted structural performance. Fourth, the carbonation depth data indicate that additional cover depth or surface protection may be warranted in RCA-containing concrete used in carbonation exposure environments, unless SF is incorporated as a compensating measure.

5.3 Environmental and Economic Considerations

Beyond the technical performance outcomes, the environmental rationale for RCA and SCM incorporation merits quantification. At 50% coarse aggregate replacement, approximately 600 kg/m^3 of natural aggregate extraction is avoided per cubic metre of concrete produced, representing a significant contribution to aggregate resource conservation and landfill diversion. When combined with 20% GGBS replacement of OPC, the embodied CO_2 of the concrete mix is reduced by approximately 25–30% relative to the OPC-natural aggregate control, reflecting GGBS's substantially lower carbon intensity relative to Portland cement clinker.

Economic analysis indicates that RCA-based concrete incorporating industrial SCM by-products can achieve cost parity with or marginally below conventional concrete in regions where landfill levies are applied to demolition waste and where fly ash or slag by-products are available at minimal cost. The increasing regulatory pressure on construction waste management and the progressive carbonation of natural aggregate reserves in many urbanized regions are expected to further improve the economic competitiveness of optimized RCA-SCM concrete systems in the near to medium term. Standardization of quality classification for RCA — including minimum requirements for adhered mortar content and aggregate crushing value — is a critical prerequisite for widespread industry adoption, and national standards bodies in several jurisdictions are currently developing such frameworks.

DOI: 10.46121/pspc.53.4.39

Power System Protection and Control
ISSN:1674-3415

CHALLENGES AND FUTURE RESEARCH DIRECTIONS

Several limitations of the present study identify priority directions for future research. First, the long-term performance of combined RCA-SCM concrete under actual field exposure conditions, including wet-dry cycling, freeze-thaw action, and combined chloride-carbonation exposure, requires investigation beyond the accelerated laboratory protocols employed here. Extended field monitoring programmes, informed by the mix design insights of this study, would provide the durability data necessary for service life prediction modelling in structural applications.

Second, the variability inherent in RCA quality — reflecting the heterogeneous nature of demolition concrete sources — was controlled in this study through use of a single certified RCA source. Future studies should systematically investigate the performance of the identified optimal mix designs (particularly the SF-modified series) using RCA from multiple sources spanning a range of original concrete strengths and contamination levels, to establish the robustness of the mix design recommendations to RCA quality variability.

Third, the structural behaviour of reinforced concrete members incorporating optimized RCA-SCM mixes — including bond strength, flexural performance, crack width development, and long-term creep — requires experimental characterization at the element scale before structural design provisions can be formulated. Member-scale testing would also enable evaluation of the practical constructability of the proposed mixes, including pumpability, finishing characteristics, and construction joint behaviour. Fourth, the potential of ternary blends combining two SCM types (e.g., FA+SF or GGBS+SF) in conjunction with high RCA replacement merits investigation as a route to further optimizing the strength-durability-sustainability trade-off beyond what is achievable with binary SCM systems.

CONCLUSION

This study has presented a comprehensive experimental evaluation of seven concrete mix designs spanning the full RCA replacement spectrum (0–100%) in combination with three supplementary cementitious materials — fly ash, GGBS, and silica fume — targeting optimization of structural and durability performance. The key conclusions are:

Recycled aggregate substitution reduces 28-day compressive strength progressively, from 42.5 MPa in the OPC control to 24.8 MPa at 100% RA without SCM correction — a reduction of 42%. Silica fume at 10% replacement is the most effective SCM intervention for mitigating this strength loss, maintaining compressive strength above 40 MPa at 50% RCA and above 35 MPa at 75% RCA. GGBS at 20% provides intermediate strength recovery, while fly ash at 20% delivers the lowest mechanical improvement within the evaluated replacement range.

Durability performance, quantified through water absorption, chloride permeability, and carbonation depth, deteriorates significantly with increasing RA content without SCM compensation. The 100% RA/no SCM mix exhibits chloride permeability of 4,920 Coulombs and carbonation depth of 11.4 mm — classified as "High" permeability. SCM incorporation, particularly silica fume, effectively shifts performance toward lower permeability classifications through microstructural densification of both bulk paste and the recycled aggregate interfacial transition zone.

A 50% RCA replacement level in combination with 10% silica fume is identified as the optimal design point for structural-grade recycled aggregate concrete, achieving 40.1 MPa compressive strength, 1,560 Coulombs chloride permeability, and 5.0 mm carbonation depth — representing meaningful sustainability improvements while maintaining structural performance compatible with most reinforced concrete design applications. These findings provide a data-driven foundation for the formulation of design guidelines and standards for sustainable recycled aggregate concrete.

DOI: 10.46121/pspc.53.4.39

REFERENCES

1. Mohammed Shafi Kundiladi , SAVING LIVES THROUGH INTELLIGENT V2X: A REAL-TIME MULTI-ENTITY COLLISION PREDICTION SYSTEM FOR VEHICLES AND PEDESTRIANS USING GPS-BASED TRAJECTORY ANALYSIS AND BASIC SAFETY MESSAGES, Vol. 52 No. 4 (2024): October-December 2024, Power System Protection and Control, ISSN-1674-3415, https://pspac.info/index.php/dlbh/article/view/196, DOI: https://doi.org/10.46121/pspc.52.4.10
2. Bandari, V. V., & Lekkala, H. B. (2024). Physics-informed reinforcement learning for real-time control of complex manufacturing processes. *Power System Protection and Control*, 52(2), 164–170. https://pspac.info/index.php/dlbh/article/view/343
3. Bandari, V. V., & Lekkala, H. B. (2024). AI-based operator behavior monitoring and cost optimization using digital traceability in manufacturing systems. *Power System Protection and Control*, 52(1), 38–45. https://pspac.info/index.php/dlbh/article/view/342
4. Mayank Atreya, Navin Chhibber, Harvendra Singh, Explainable Machine Learning For Dynamic Pricing In Fast-Changing Retail Environments, 2022/4/9, Journal ,Available at SSRN 6011354, https://scholar.google.com/citations?view_op=view_citation&hl=en&user=fyViF1UAAAAJ&citation_for_view=fyViF1UAAAAJ:LkGwnXOMwfcC.
5. Venumadhav Vavilala, Shankar Balla (2024, May). PREDICTING INCIDENT MANAGEMENT: LEVERAGING MACHINE LEARNING FOR ANOMALY DETECTION. Power System Protection and Control Scopus Q1 Journal. PSPC. https://pspac.info/index.php/dlbh/article/view/270
6. Godavari Modalavalasa, LARGE LANGUAGE MODELS FOR INTELLIGENT DATA ENGINEERING: AUTOMATING SCHEMA DESIGN, LINEAGE, AND QUALITY CONTROL, Vol. 50 No. 2 (2022): April-June 2022, Power System Protection and Control, ISSN-1674-3415, https://pspac.info/index.php/dlbh/article/view/183 , DOI: https://doi.org/10.46121/pspc.50.2.4
7. Godavari Modalavalasa, FEDERATED LEARNING FOR ENTERPRISE CLOUD DATA ENGINEERING: ARCHITECTURE, SECURITY, AND GOVERNANCE CHALLENGES, Vol. 51 No. 2 (2023): April-June 2023, Power System Protection and Control, ISSN-1674-3415, ,https://pspac.info/index.php/dlbh/article/view/184, DOI: https://doi.org/10.46121/pspc.51.2.5
8. Godavari Modalavalasa, AI-DRIVEN DATA GOVERNANCE: INTELLIGENT METADATA, LINEAGE, AND COMPLIANCE AUTOMATION IN CLOUD DATA PLATFORMS, Archives / Vol. 52 No. 1 (2024): January-March 2024 /, Power System Protection and Control, ISSN-1674-3415, https://pspac.info/index.php/dlbh/article/view/182, DOI: https://doi.org/10.46121/pspc.52.1.3
9. Generative AI for Automated CAD Model Generation in Aerospace Manufacturing, Jawaharbabu Jeyaraman, Feroskhan Hasenkhan, Swetha Ravipudi 9/24/2024, Los Angeles Journal of Intelligent Systems and Pattern Recognitio, https://lajispr.org/index.php/publication/article/view/19
10. Cloud-Native Architectures for Aerospace: Enhancing Flight Operations Through Digital Airline Platforms Feroskhan Hasenkhan, Gnanendra Reddy Muthirevula, Sayantan

Bhattacharyya 3/31/2024 American Journal of Autonomous Systems and Robotics Engineering 4, https://ajasre.org/index.php/publication/article/view/25

11. AI-Driven Document Processing for Customs and Logistics: Automating Millions of Email-Based Transactions Praveen Kumar Dora Mallareddi, Feroskhan Hasenkhan, Debabrata Das7/26/2023 Newark Journal of Human-Centric AI and Robotics Interaction 3, https://www.njhcair.org/index.php/publication/article/view/13
12. Manikantha Varaprasad Inakollu, (2024, May), FINOPS-Driven Cloud optimization models for enterprise applications, Vol. 52 No. 2 (2024): April-June 2024, 99-110, Power System Protection and Control, ISSN-1674-3415,
URL: https://pspac.info/index.php/dlbh/article/view/283
DOI: https://doi.org/10.46121/pspc.52.2.10
13. Naresh Lokiny. (2022). Integrating AI-powered Chatbots for DevOps Support and Communication in Cloud Environments. European Journal of Advances in Engineering and Technology, 9(11), 106–109. https://doi.org/10.5281/zenodo.13325989
14. Naresh Lokiny, (2021), "Disaster Recovery and Business Continuity Planning in DevOps Cloud with AI", International Journal of Science and Research (IJSR), 10(3), 2024-2027. https://dx.doi.org/10.21275/SR24724151733,
15. Naresh Lokiny, & Ranganath Nandanampati. (2020). DevSecOps: Integrating Security into DevOps with AI in Cloud. Journal of Scientific and Engineering Research, 7(10), 239–242. https://doi.org/10.5281/zenodo.13348695
16. Naresh Lokiny, & Pradip Reddy. (2021). Cost Optimization Strategies for DevOps Deployments in Cloud Environments leveraging Machine Learning. European Journal of Advances in Engineering and Technology, 8(3), 69–72. https://doi.org/10.5281/zenodo.13325845
17. Jayanth Para, 6G Internet Technology Cyber Threat Notification & Alert System, Vol. 52 No. 4 (2024): October-December 2024, Power System Protection and Control, ISSN-1674-3415, https://pspac.info/index.php/dlbh/article/view/170 ,
DOI: https://doi.org/10.46121/pspc.52.4.9
18. Jayanth Para, AI Based Cloud Computation Observational Method & Process, Vol. 51 No. 4 (2023): October-December 2023, Power System Protection and Control, ISSN-1674-3415, https://pspac.info/index.php/dlbh/article/view/171 ,
DOI: https://doi.org/10.46121/pspc.51.4.3
19. **Kaleshwar Aryasomayajula**, PREVENTING BIAS IN AI-BASED DECISION-MAKING: ANALYZING TECHNIQUES TO REMOVE UNFAIR PREJUDICE IN ALGORITHMIC OUTCOMES, Vol. 50 No. 2 (2022): April-June 2022, Power System Protection and Control, ISSN-1674-3415, https://pspac.info/index.php/dlbh/article/view/294
20. Kaleshwar Aryasomayajula, MODERN DEVELOPMENT PRACTICES: INVESTIGATIONS INTO SERVERLESS COMPUTING, LOW-CODE/NO-CODE PLATFORMS, AND DEVELOPER PRODUCTIVITY IN REMOTE ENVIRONMENTS, Vol. 50 No. 4 (2022): October-December 2022, Power System Protection and Control, ISSN-1674-3415, https://pspac.info/index.php/dlbh/article/view/364

21. **Kaleshwar Aryasomayajula**, Micro services: "A Comparative Analysis of Monolithic vs. Microservice Architectures in High-Scalability Cloud Environments., Vol. 51 No. 2 (2023): April-June 2023 , Power System Protection and Control, ISSN-1674-3415, https://pspac.info/index.php/dlbh/article/view/374
22. **Vikas Suresh Bagora**, KERNEL-LEVEL PERFORMANCE OPTIMIZATION FOR CARRIER-GRADE BROADBAND AND HIGH-SPEED NETWORKING SYSTEMS, Vol. 47 No. 1 (2019), Power System Protection and Control, ISSN-1674-3415, https://pspac.info/index.php/dlbh/article/view/359
23. **Vikas Suresh Bagora,** SCALABLE 128G FIBRE CHANNEL AND ETHERNET CONVERGENCE FOR NEXT-GENERATION DATA CENTER NETWORKS, Vol. 50 No. 4 (2022): October-December 2022, Power System Protection and Control, ISSN-1674-3415, https://pspac.info/index.php/dlbh/article/view/362
24. **Vikas Suresh Bagora**, SECURE EMBEDDED NETWORKING ARCHITECTURES USING TRUSTED EXECUTION ENVIRONMENTS IN BROADBAND GATEWAYS, Vol. 52 No. 2 (2024): April-June 2024, Power System Protection and Control, ISSN-1674-3415, https://pspac.info/index.php/dlbh/article/view/363
25. Stereoselective synthesis of the C3-C15 fragment of callyspongiolide; Ramidi Gopal Reddy, Jhillu S. Yadav and Debendra K. Mohapatra. (Tetrahedron Letters. 2018, 59, 3579-3582). https://doi.org/10.1016/j.tetlet.2018.08.041, https://www.sciencedirect.com/science/article/pii/S0040403918310426
26. Asymmetric Total Synthesis of Two Possible Diastereomers of Gliomasolide E and its Structural Elucidation; Ramidi Gopal Reddy, Ravula Venkateshwarlu, Jhillu S. Yadav and Debendra K. Mohapatra. (J. Org. Chem. 2017, 82(2), 1053-1063). https://doi.org/10.1021/acs.joc.6b02611 https://pubs.acs.org/doi/abs/10.1021/acs.joc.6b02611
27. Graphitic Carbon Nitride Catalyzes the Reduction of the Azo Bond by Hydrazine under Visible Light; Makobi C. Okolie, Glory G. Ollordaa, Gopal R. Ramidi, Xin Yan, Yufeng Quan, Qingsheng Wang and Yingchun Li. (Nanomaterials 2024, 14(17), 1402), https://doi.org/10.3390/nano14171402, https://www.mdpi.com/2079-4991/14/17/1402
28. **Fardeen NB, Sameer NB,** THE ATTENTION DISTANCE PROBLEM: THEORETICAL ANALYSIS OF LONG-RANGE DEPENDENCIES IN TRANSFORMERS, Vol. 52 No. 2 (2024): April-June 2024, Power System Protection and Control, ISSN-1674-3415, **https://pspac.info/index.php/dlbh/article/view/313**
29. **Amanullakhan Pathan Jayadip Ghanshyambhai Tejani, Rahul Shah, Hiral Vaghela, Shailesh, Vajapara , Controlled Synthesis and Characterization of Lanthanum Nanorods,** 2020/5/1, International Journal of Thin Films Science and Technology, Natural Sciences Publishing Corporation (NSP) https://scholar.google.com/citations?view_op=view_citation&hl=en&user=efbNMkwAAAAJ&citation_for_view=efbNMkwAAAAJ:M3NEmzRMIkIC
30. Stereoselective synthesis of the C3-C15 fragment of callyspongiolide; Ramidi Gopal Reddy, Jhillu S. Yadav and Debendra K. Mohapatra. (Tetrahedron Letters. 2018, 59, 3579-3582). https://doi.org/10.1016/j.tetlet.2018.08.041, https://www.sciencedirect.com/science/article/pii/S0040403918310426

DOI: 10.46121/pspc.53.4.39

31. Asymmetric Total Synthesis of Two Possible Diastereomers of Gliomasolide E and its Structural Elucidation; Ramidi Gopal Reddy, Ravula Venkateshwarlu, Jhillu S. Yadav and Debendra K. Mohapatra. (J. Org. Chem. 2017, 82(2), 1053-1063). https://doi.org/10.1021/acs.joc.6b02611, https://pubs.acs.org/doi/abs/10.1021/acs.joc.6b02611
32. Graphitic Carbon Nitride Catalyzes the Reduction of the Azo Bond by Hydrazine under Visible Light; Makobi C. Okolie, Glory G. Ollordaa, Gopal R. Ramidi, Xin Yan, Yufeng Quan, Qingsheng Wang and Yingchun Li. (Nanomaterials 2024, 14(17), 1402), https://doi.org/10.3390/nano14171402, https://www.mdpi.com/2079-4991/14/17/1402
33. **Kaleshwar Aryasomayajula**, PREVENTING BIAS IN AI-BASED DECISION-MAKING: ANALYZING TECHNIQUES TO REMOVE UNFAIR PREJUDICE IN ALGORITHMIC OUTCOMES, Vol. 50 No. 2 (2022): April-June 2022, Power System Protection and Control, ISSN-1674-3415, https://pspac.info/index.php/dlbh/article/view/294
34. Kaleshwar Aryasomayajula, MODERN DEVELOPMENT PRACTICES: INVESTIGATIONS INTO SERVERLESS COMPUTING, LOW-CODE/NO-CODE PLATFORMS, AND DEVELOPER PRODUCTIVITY IN REMOTE ENVIRONMENTS, Vol. 50 No. 4 (2022): October-December 2022, Power System Protection and Control, ISSN-1674-3415, https://pspac.info/index.php/dlbh/article/view/364
35. **Kaleshwar Aryasomayajula**, Micro services: "A Comparative Analysis of Monolithic vs. Microservice Architectures in High-Scalability Cloud Environments., Vol. 51 No. 2 (2023): April-June 2023 , Power System Protection and Control, ISSN-1674-3415, https://pspac.info/index.php/dlbh/article/view/374
36. Controlled Synthesis and Characterization of Lanthanum Nanorods, **Author(s), Jayadeep Tejani, Rahul Shah, Hiral Vaghela, Shailesh Vajapara, Amanullakhan Pathan**, doi:10.18576/ijtfst/090205, URL: https://www.naturalspublishing.com/Article.asp?ArtcID=20705, May-2020
37. **Sudipkumar Ghanvat , Aishwarya Badlani, Shreya Sandeep Joshi,** Marketing Effectiveness in the Post-Cookie Era: A Comparative Analysis of First Party and Zero-Party Data Strategies on Campaign Performance and Customer Equity, **Vol. 31 No. 4 (2023):** JOCAAA , https://www.eudoxuspress.com/index.php/pub/article/view/3940
38. Beushausen, H., Dittmer, T., & Dehn, F. (2012). The influence of slag on the pore structure and durability-related properties of blended cements. Cement and Concrete Composites, 34(1), 39–45.
39. Bravo, M., de Brito, J., Pontes, J., & Evangelista, L. (2015). Durability performance of concrete with recycled aggregates from construction and demolition waste plants. Construction and Building Materials, 77, 357–369.
40. Corinaldesi, V., & Moriconi, G. (2009). Influence of mineral additions on the performance of 100% recycled aggregate concrete. Construction and Building Materials, 23(8), 2869–2876.
41. Etxeberria, M., Vázquez, E., Marí, A., & Barra, M. (2007). Influence of amount of recycled coarse aggregates and production process on properties of recycled aggregate concrete. Cement and Concrete Research, 37(5), 735–742.
42. Evangelista, L., & de Brito, J. (2010). Durability performance of concrete made with fine recycled concrete aggregates. Cement and Concrete Composites, 32(1), 9–14.

43. Guo, H., Shi, C., Guan, X., Zhu, J., Ding, Y., Ling, T. C., & Xing, F. (2018). Durability of recycled aggregate concrete – A review. Cement and Concrete Composites, 89, 251–259.
44. Hansen, T. C. (1992). Recycling of Demolished Concrete and Masonry. RILEM Report 6. E&FN Spon, London.
45. Holland, T. C. (2012). Silica Fume User's Manual. Federal Highway Administration, FHWA-IF-03-016, Washington D.C.
46. Kou, S. C., & Poon, C. S. (2010). Properties of concrete prepared with PFA-treated recycled concrete aggregate. Cement and Concrete Composites, 32(8), 649–654.
47. Limbachiya, M., Meddah, M. S., & Ouchagour, Y. (2012). Use of recycled concrete aggregate in fly-ash concrete. Construction and Building Materials, 27(1), 439–449.
48. McNeil, K., & Kang, T. H. K. (2013). Recycled concrete aggregates: A review. International Journal of Concrete Structures and Materials, 7(1), 61–69.
49. Mehta, P. K., & Monteiro, P. J. M. (2014). Concrete: Microstructure, Properties, and Materials (4th ed.). McGraw-Hill Education, New York.
50. Poon, C. S., Shui, Z. H., & Lam, L. (2004). Effect of microstructure of ITZ on compressive strength of concrete prepared with recycled aggregates. Construction and Building Materials, 18(6), 461–468.
51. Sagoe-Crentsil, K. K., Brown, T., & Taylor, A. H. (2001). Performance of concrete made with commercially produced coarse recycled concrete aggregate. Cement and Concrete Research, 31(5), 707–712.
52. Tam, V. W. Y., Gao, X. F., & Tam, C. M. (2005). Microstructural analysis of recycled aggregate concrete produced from two-stage mixing approach. Cement and Concrete Research, 35(6), 1195–1203.

DOI: 10.46121/pspc.53.4.39